Polarization-dependent fluorescence from an anisotropic gold/polymer hybrid nano-emitter

X. Zhou, C. Deeb, R. Vincent, T. Lerond, P.-M. Adam, J. Plain, G. P. Wiederrecht, F. Charra, C. Fiorini, G. Colas des Francs, O. Soppera, and R. Bachelot

---

Polarization-dependent fluorescence from an anisotropic gold/polymer hybrid nano-emitter

X. Zhou,[1] C. Deeb,[1,a)] R. Vincent,[1] T. Lerond,[1] P.-M. Adam,[1] J. Plain,[1] G. P. Wiederrecht,[2] F. Charra,[3] C. Fiorini,[3] G. Colas des Francs,[4] O. Soppera,[5] and R. Bachelot[1,b)]

[1]*Institut Charles Delaunay-Laboratoire de Nanotechnologie et d'Instrumentation Optique (ICD-LNIO), CNRS UMR 6279, Université de Technologie de Troyes, 12 Rue Marie Curie CS 42060, 10004 Troyes Cedex, France*
[2]*Center for Nanoscale Materials, Argonne National Laboratory, Argonne, Illinois 60439, USA*
[3]*CEA/IRAMIS/Service de Physique et Chimie des Surfaes et Interfaces, Centre d'Etudes de Saclay, F91191 Gif-sur-Yvette Cedex, France*
[4]*Laboratoire Interdisciplinaire Carnot de Bourgogne (ICB), Université de Bourgogne, 9 av. A. Savary 21078, Dijon, France*
[5]*Institut de Science des Matériaux de Mulhouse IS2M, CNRS UMR 7361, Université de Haute-Alsace, Mulhouse, France*

Based on nanoscale photopolymerization triggered by the dipolar surface plasmon mode, we developed a light-emitting gold nanoparticle/Eosin Y-doped polymer hybrid nanostructure. Due to the anisotropic spatial distribution of the dipolar surface plasmon mode during photopolymerization, this nano-emitter is anisotropic in both geometry and emission. The trapped dye molecules in the hybrid nanostructure display fluorescence intensity that is dependent upon the polarization of the incident excitation light. This nano-emitter further allows the photo-selection of fluorescence configuration (i.e., molecule concentration and refractive index of active medium) by controlling the incident polarization. © 2014 AIP Publishing LLC. [http://dx.doi.org/10.1063/1.4861898]

The field of hybrid plasmonics has made significant contributions to our understanding of interactions between metals and other materials in the sub-wavelength regime. The metal nanostructure that supports surface plasmons can be combined with other materials such as semiconductors,[1,2] organic dyes,[3–5] biomolecules,[6] and inorganic components.[7,8] Such a hybrid configuration benefits from the different properties of each of its constituents for fascinating applications such as biological and chemical sensors,[9–11] hybrid nanoparticles with widely tunable plasmon resonances,[12–14] as well as metal/fluorophore nano-emitters (NEs).[15,16]

Many different processes have been developed for synthesizing a hybrid configuration. Typically, a layer of dye molecules is coated homogeneously on the entire sample of the metallic nanostructures,[5,17,18] and the emission of molecules that are distributed in the vicinity of the nanoparticles are significantly modified. Biomolecules such as DNA chains can also be applied to bind fluorophores close to metal nanoparticles (MNPs).[19,20] Moreover, homogeneous dye-doped-shells can be fabricated to surround the nanoparticles to form a core/shell configuration.[15,21] All of these approaches provided good results in the reported studies. However, for the case of NEs, the homogeneous dye distribution prevents the photo-selection of any specific fluorescence configuration (defined as molecule population and refractive index of active medium in this Letter) of the hybrid NE using the polarization of incident light, unless different plasmon modes of the MNP are excited.[21] In other words, integration of the active medium has been so far isotropic. An anisotropic hybrid plasmonic NE based on the inhomogeneous spatial distribution of the active medium has not yet been reported.

In this Letter, we present a light-emitting hybrid plasmonic nanostructure with an anisotropic dye-containing photopolymer nanostructure surrounding the gold nanoparticle (GNP) in order to make the fluorescence controllable by incident polarization. This idea was recently suggested in a patent.[22] The present Letter reports an experimental demonstration. To confirm the anisotropic nature of our gold/polymer hybrid system, gold nanospheres were used in this study. The hybrid system was characterized with atomic force microscopy (AFM) and fluorescence spectroscopy. By rotating the polarization of the excitation light, different fluorescence configurations of the NE can be photo-selected, resulting in different fluorescence intensities.

An aqueous solution of gold nanospheres with diameters of about 70 nm and a concentration of $4.8 \times 10^{12} l^{-1}$ was synthesized following a seed-mediated method introduced by Murphy and coworkers.[23] To recognize a certain nanoparticle from the numerous randomly distributed colloids, gold landmarks were fabricated on the glass substrate by electron-beam lithography. The substrate with landmarks was then functionalized by 3-aminopropyltriethoxysilane. Afterwards, the substrate was dip-coated in the gold colloids for 1.5 h. It was then rinsed with deionized water and dried with air. Fig. 1(a) shows a region of the sample characterized by AFM. The area within a pair of L-shaped landmarks is $5.5 \times 5.5 \mu m^2$. Fig. 1(b) shows an example of the scattering spectrum of a single gold nanosphere selected. It presents a peak at 580 nm.

The light-emitting GNP/polymer hybrid nanostructure was fabricated based on a nanoscale photopolymerization process that was triggered by the surface plasmon-enhanced local optical electromagnetic field.[24–28] The radical-free
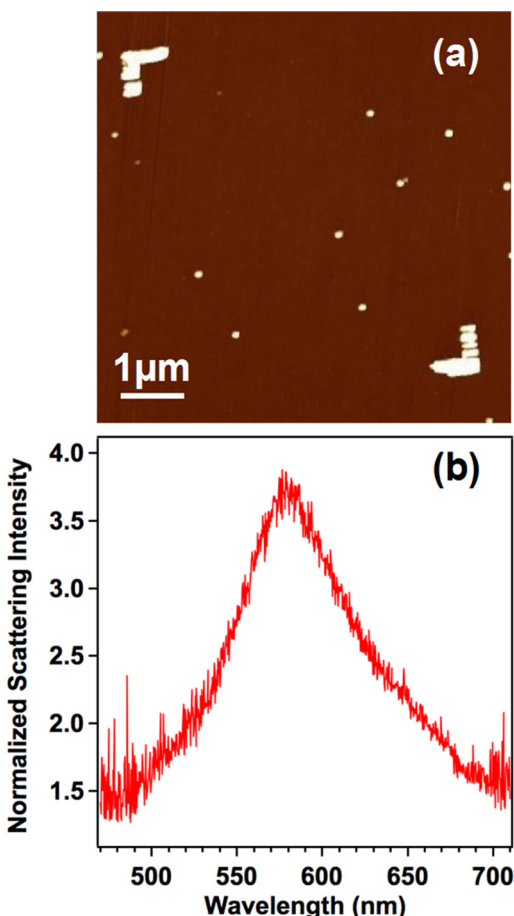
FIG. 1. (a) AFM image of a $5.5 \times 5.5 \, \mu m^2$ region of the sample and (b) scattering spectrum from an individual gold nanosphere.

FIG. 2. (a) Differential AFM image of a unique GNP/polymer hybrid structure. The diameter of the gold nanosphere is 70 nm. $\mathbf{E_0}$ illustrates the polarization of incident laser for photopolymerization. (b) The cross-section profiles of the differential AFM image across the center of the nanosphere along X (dashed line) and Y (solid line) axes.

photopolymerizable solution utilized for the photopolymerization was made up of 96 wt.% pentaerythritol triacrylate (PETIA), 4 wt.% methyldiethanolamine (MDEA), and 0.5 wt.% Eosin Y (EY). The solution has a threshold dose for photopolymerization, so that polymer structures can be selectively integrated in the vicinity of metal nanosphere where the local dose related to the optical near-field exceeds the threshold *via* plasmon enhancement. After being coated with the polymerizable solution, the nanoparticle sample was irradiated by a $\lambda_0 = 532$ nm linearly polarized laser. The incident dose was set at 70% of the threshold to prevent photopolymerization in the far-field. Along the polarization direction in the vicinity of the nanoparticles, the local field was enhanced by the excited surface plasmon to exceed the polymerization threshold. After irradiation, the unpolymerized solution was removed by rinsing with chloroform and isopropanol. The nano-object was characterized by AFM before and after the photopolymerization. The difference between AFM images taken before and after the photopolymerization highlights the polymer structures of the hybrid NE. Fig. 2(a) shows a typical differential AFM image of a unique hybrid structure. It is obtained from the AFM image that is collected before the photopolymerization subtracted from the image taken after the procedure. The integrated polymer nanostructures are highlighted and the shadow in the center corresponds to the initial gold nanosphere. Fig. 2(b) illustrates the cross-section profiles of the differential AFM image of the hybrid nanostructure along X-axis
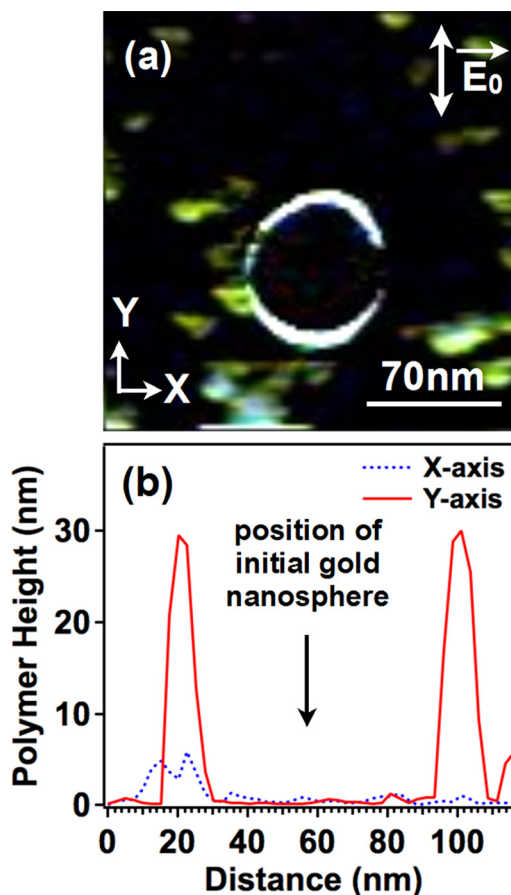
(dashed blue line) and Y-axis (solid red line) across the spherical center. The two peaks of the Y-axis profile represent the integrated polymer whose size can be read from the profile (15 nm on average). As is pointed out by the arrow, the valley between the peaks corresponds to the position of the initial gold nanosphere. According to the profile along the X-axis, some residual features from the polymerizable solution can be found on the substrate. They have, however, a height much lower than the integrated polymer structures. Fig. 2 well illustrates the anisotropic nature of the EY-containing active medium integrated to the isotropic gold nanosphere. It should be stressed that this anisotropy is the reflection of the anisotropy of the plasmon dipolar mode used for photopolymerization.[25]

EY molecules outside of the polymer nanostructures were mostly removed by rinsing, while those in the volume of the plasmon field were trapped in the polymer. The dipolar distribution of the EY-doped polymer makes the hybrid nanostructure an anisotropic NE that allows photo-selection of fluorescence configuration by the polarization of excitation light. With an excitation wavelength of $\lambda_{ex} = 514$ nm, fluorescence signals from EY were collected from the hybrid structure whose profile is in Fig. 2. An inverse microscope with an objective of $40 \times / 0.6$ NA was utilized for both excitation and collection. The diameter of the incident laser beam at the focus was about $1 \, \mu m$. A band-pass filter was

used to select the emission in the 530–570 nm range and sub-sequently focused into a spectrometer.

To demonstrate the polarization-dependent emission signal of a unique NE, two different incident polarizations, along the X-axis and Y-axis, were utilized. Correspondingly, we define the fluorescence spectra (see also the schemes in Fig. 3):

- S_x: fluorescent signal excited with an incident polarization along the X-axis (Fig. 3(a)). The near-field is perpendicular to the dye-doped polymer lobes.
- S_y: fluorescent signal excited with an incident polarization along the Y-axis (Fig. 3(b)). The near-field overlaps with the polymer.

Four positions of dye molecules were considered (see Fig. 3): (1) molecule one constitutes reference signal (RF) far from the nanostructure (i.e., emitters far from the plasmonic nano-sources); (2) outside the polymer but close to the nanoparticle; (3) inside the polymer and can be enhanced by applying either X or Y incident polarization; and (4) inside the polymer and can be activated by the near-field only with Y polarization. The concentration of molecules at positions 3 and 4 is higher than positions 1 and 2. Let us point out that molecules 1 and 2 are expected to be rinsed out and their presence is thus unlikely.

Fig. 4(a) illustrates the fluorescence of EY molecules from a single NE under the two different incident polarizations. The acquisition time for each spectrum was 15 s. The spectra were collected in a chronological order of a-b-c in the legend. In other words, we started with an incident polarization along X-axis (aS_x). Emission of EY molecules at positions 2 and 3 can be enhanced by the plasmon near-field. Then an incident polarization along the polymer lobes (bS_y) was used. In this situation, molecules at positions 3 and 4 are excited by the near-field. To reproduce the result, the

FIG. 4. (a) Fluorescent signals from the NE collected with different incident polarizations. The reference signal (RF) was collected 2-μm away from the NE on the substrate. Positions of molecules involved are identified by the numbers 1, 2, 3, and 4. (b) Differential fluorescent spectra of "S_y-S_x" for both NE and RF.

polarization was rotated back to X-axis (cS_x). We oriented the sample by 90° to "rotate the incident polarization" in order to avoid any difference arisen from the polarization sensitivity of the optical system. Signals from the substrate (2-μm away from the NE, represented by position 1) were collected as a reference (RF).

Fig. 4(a) provides three primary pieces of information about the NE. First, the reference signal (RF) has an intensity of 68 counts. This indicates that some EY molecules (labeled "1" in Fig. 3(a)) remain on the substrate despite the rinsing process. However, as will be discussed in Fig. 4(b), these molecules do not contribute to the anisotropic fluorescence of the NE. Second, the S_x signal collected from the NE (115 counts) is significantly higher than the RF. Considering the concentration of dye molecules at position 2 is same as that of position 1, illustrated in Fig. 3, this 1.7-times enhancement is likely to be resulted from the modification of fluorescence by a GNP. Such a low enhancement has been observed in some other studies based on simple MNPs.[29,30] In our study, it is due to the weak coupling of incident excitation field and emission wavelength to the plasmon resonance of dipolar mode of the gold nanosphere. Let us point out that molecule 3 contributed as well to this enhancement. Third, we obtained from the NE a S_y (170 counts)
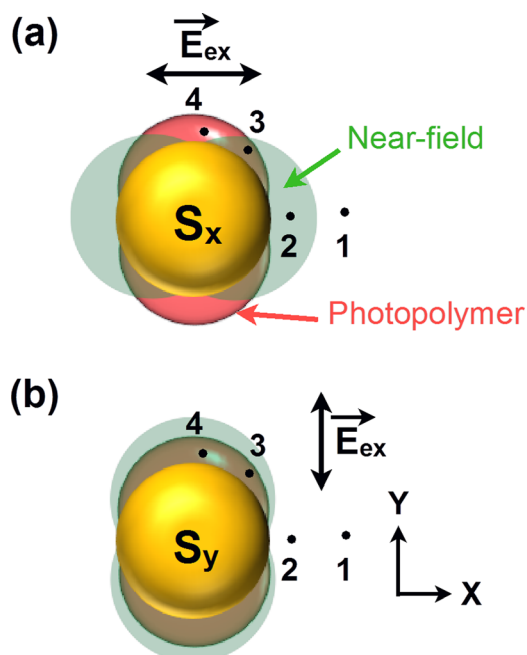

FIG. 3. Scheme of the two configurations for fluorescence signals from the NE (a) S_x, with an incident polarization along the X-axis and (b) S_y, with an incident polarization along the Y-axis.
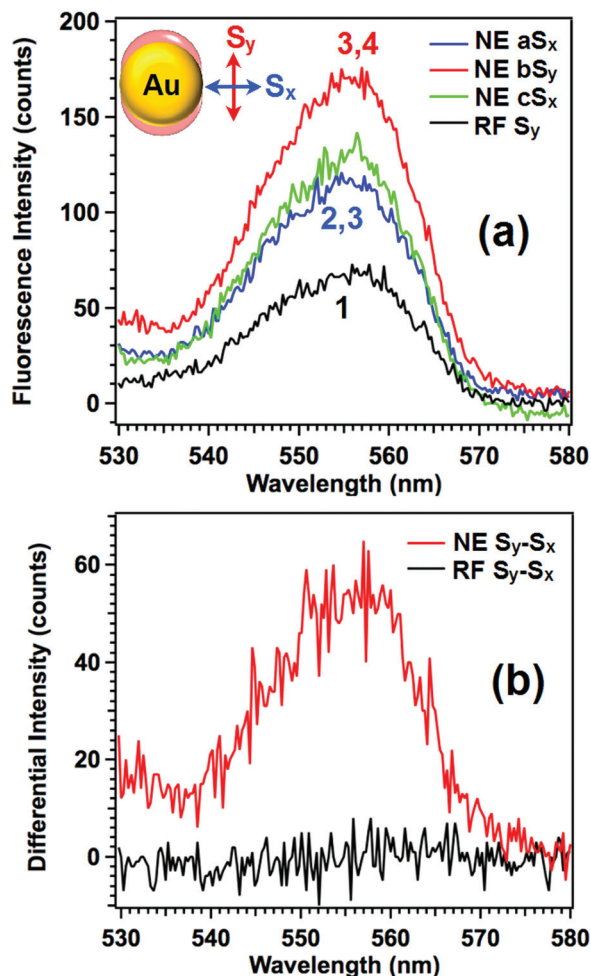
higher than S_x. The anisotropy of our hybrid NE can be described by the ratio of RF-corrected fluorescence intensities. $(S_y - RF)/(S_x - RF) \approx 2.2$. This ratio results from the larger number of molecules (molecules "4" mainly involved) that are excited when the incident polarization produces a near-field that overlaps the dye-doped polymer. Besides, the anisotropy of the NE can be highlighted by comparing the differential spectra "S_y-S_x" (Fig. 4(b)) on the NE and on the substrate. Let us point out that signal from molecule 3 has been canceled out in the differential spectrum, because it contributed in the same way for both S_x and S_y. The reference fluorescence signal shows no polarization dependence, while a positive result from NE indicates the polarization sensitivity of the anisotropic hybrid NE.

Our NE has a complex configuration with an anisotropic distribution of dye-doped polymer. We performed a simple yet representative calculation based on Mie theory on the normalized fluorescence intensity I/I_0 for a single molecule, with I_0 and I the fluorescence intensity of a single molecule in free space and close to a MNP, respectively. An average molecular orientation was adopted because the local dipole orientation was not controllable in our experiment. More details regarding the calculation can be found in references.[31–34] The calculation was performed in an isotropic medium of n = 1.48, corresponding to the thin organic shell (n = 1.48) surrounding molecules 1 and 2 despite rinsing, and polymer structures (n = 1.52) that host molecules 3 and 4. The calculated map of the normalized fluorescence intensity is shown in Fig. 5, with cross-sections in the (a) XZ plane and (b) XY plane across the particle center.

The calculation demonstrates the anisotropy introduced by the excitation field. The maximum fluorescence poles tilt towards the positive Z-axis due to the slight excitation of quadrupolar plasmon modes. The cross-section in XY plane (Fig. 5(b)) shows that the maximum fluorescence poles oriented along the incident polarization. The calculated normalized fluorescence intensity presented a maximum of 1.45. The experimental results of "*NE S_x/RF = 1.7*" and "NE S_y/RF = 2.5*", however, indicate extra-enhancements that come mainly from (i) the higher molecule concentration within the polymer nanostructures (positions 3 and 4) than on the substrate (positions 1 and 2), which is not yet included in the model and (ii) the overlapping of plasmon field with the higher concentration of dye molecules. The theoretical calculation thus helps in confirming the anisotropy of our hybrid NE.

To sum up, we report in this Letter a spatially anisotropic nano-emitter produced via photopolymerization that is triggered by the dipolar plasmon enhancement of the electromagnetic near-field supported by a gold nanosphere. Greater fluorescence was reproducibly detected with an incident polarization along the long axis of the hybrid nano-emitter than that along the short axis. The fluorescence intensity is highly controllable with the polarization of the excitation laser. These results have been reproduced for many 70-nm diameter gold spheres. Calculations further support the spatial anisotropy of the emission and quantitate the rate of emission enhancement as a function of the dye molecule-metal surface distance. These results demonstrate the potential utility of a spatially anisotropic hybrid nano-emitter for nanophotonics applications.
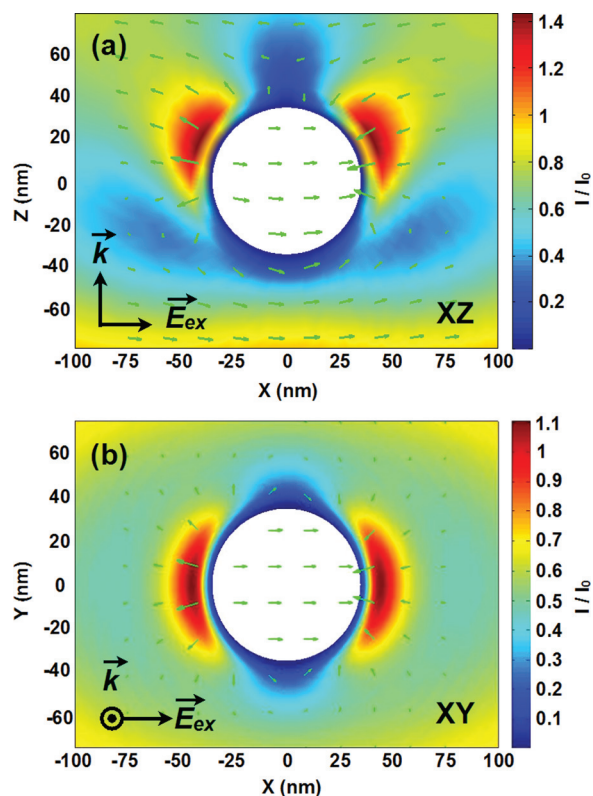

FIG. 5. Spatial distribution of the orientation-averaged normalized fluorescence intensity I/I_0 of single EY molecule near a gold nanosphere (i.e., fluorescence intensity as a function of the spatial position of the molecule). Profiles in the (a) XZ plane and (b) XY plane across the center of the nanosphere. Calculation was performed in an isotropic medium of n = 1.48 with an excitation wavelength of $\lambda_{ex} = 514$ nm and an emission wavelength of $\lambda_{em} = 555$ nm. Incident light propagates in the direction of the positive Z-axis and polarized along X-axis. Green arrows represent the electric field orientations.

[1]A. G. Curto, G. Volpe, T. H. Taminiau, M. P. Kreuzer, R. Quidant, and N. F. van Hulst, Science **329**, 930 (2010).
[2]O. Kulakovich, N. Strekal, A. Yaroshevich, S. Maskevich, S. Gaponenko, I. Nabiev, U. Woggon, and M. Artemyev, Nano Lett. **2**, 1449 (2002).
[3]W. Zhou, M. Dridi, J. Y. Suh, C. H. Kim, D. T. Co, M. R. Wasielewski, G. C. Schatz, and T. W. Odom, Nat. Nanotechnol. **8**, 506 (2013).
[4]T. Sen and A. Patra, J. Phys. Chem. C **116**, 17307 (2012).
[5]A. Kinkhabwala, Z. Yu, S. Fan, Y. Avlasevich, K. Müllen, and W. E. Moerner, Nat. Photonics **3**, 654 (2009).
[6]W. P. Hall, S. N. Ngatia, and R. P. Van Duyne, J. Phys. Chem. C **115**, 1410 (2011).
[7]A. Furube, L. Du, K. Hara, R. Katoh, and M. Tachiya, J. Am. Chem. Soc. **129**, 14852 (2007).
[8]H. Cong, R. Toftegaard, J. Arnbjerg, and P. R. Ogilby, Langmuir **26**, 4188 (2010).
[9]K. M. Mayer, S. Lee, H. Liao, B. C. Rostro, A. Fuentes, P. T. Scully, C. L. Nehl, and J. H. Hafner, ACS Nano **2**, 687 (2008).
[10]Z.-Y. Li and Y. Xia, Nano Lett. **10**, 243 (2010).

[11]R. L. Truby, S. Y. Emelianov, and K. A. Homan, Langmuir **29**, 2465 (2013).

[12]J. Li, S. K. Cushing, J. Bright, F. Meng, T. R. Senty, P. Zheng, A. D. Bristow, and N. Wu, ACS Catal. **3**, 47 (2013).

[13]C. Wu and Q.-H. Xu, Langmuir **25**, 9441 (2009).

[14]H. Wang, D. W. Brandl, F. Le, P. Nordlander, and N. J. Halas, Nano Lett. **6**, 827 (2006).

[15]M. A. Noginov, G. Zhu, A. M. Belgrave, R. Bakker, V. M. Shalaev, E. E. Narimanov, S. Stout, E. Herz, T. Suteewong, and U. Wiesner, Nature **460**, 1110 (2009).

[16]L. Zhao, T. Ming, L. Shao, H. Chen, and J. Wang, J. Phys. Chem. C **116**, 8287 (2012).

[17]Y. Leroux, E. Eang, C. Fave, G. Trippe, and J. C. Lacroix, Electrochem. Commun. **9**, 1258 (2007).

[18]Y. Chen, K. Munechika, I. J.-L. Plante, A. M. Munro, S. E. Skrabalak, Y. Xia, and D. S. Ginger, Appl. Phys. Lett. **93**, 053106 (2008).

[19]E. Dulkeith, M. Ringler, T. A. Klar, and J. Feldmann, Nano Lett. **5**, 585 (2005).

[20]Z. Gueroui and A. Libchaber, Phys. Rev. Lett. **93**, 166108 (2004).

[21]T. Ming, L. Zhao, Z. Yang, H. Chen, L. Sun, J. Wang, and C. Yan, Nano. Lett. **9**, 3896 (2009).

[22]F. Charra, C. Fiorini, and R. Bachelot, "Laser plasmonique et son procedé de fabrication," Patent EPRmn263/432FR (11 March 2011).

[23]N. R. Jana, L. Gearheart, and C. J. Murphy, Chem. Mater. **13**, 2313 (2001).

[24]H. Ibn El Ahrach, R. Bachelot, A. Vial, G. Lérondel, J. Plain, and P. Royer, Phys. Rev. Lett. **98**, 107402 (2007).

[25]C. Deeb, R. Bachelot, J. Plain, A.-L. Baudrion, S. Jradi, A. Bouhelier, O. Soppera, P. K. Jain, L. Huang, C. Ecoffet, L. Balan, and P. Royer, ACS Nano **4**, 4579 (2010).

[26]C. Deeb, C. Ecoffet, R. Bachelot, J. Plain, A. Bouhelier, and O. Soppera, J. Am. Chem. Soc. **133**, 10535 (2011).

[27]C. Deeb, X. Zhou, D. Gérard, A. Bouhelier, P. K. Jain, J. Plain, O. Soppera, P. Royer, and R. Bachelot, J. Phys. Chem. Lett. **2**, 7 (2011).

[28]C. Deeb, X. Zhou, R. Miller, S. K. Gray, S. Marguet, J. Plain, G. P. Wiederrecht, and R. Bachelot, J. Phys. Chem. C **116**, 24734 (2012).

[29]L. Dong, F. Ye, A. Chughtai, S. Popov, A. T. Friberg, and M. Muhammed, Opt. Lett. **37**, 34 (2012).

[30]L. Dong, F. Ye, A. Chughtai, V. Liuolia, S. Popov, A. T. Friberg, and M. Muhammed, IEEE J. Quantum Electron. **48**, 1220 (2012).

[31]P. Anger, P. Bharadwaj, and L. Novotny, Phys. Rev. Lett. **96**, 113002 (2006).

[32]Y. S. Kim, P. T. Leung, and T. F. George, Surf. Sci. **195**, 1 (1988).

[33]G. Colas des Francs, A. Bouhelier, E. Finot, J.-C. Weeber, A. Dereux, and E. Dujardin, Opt. Express. **16**, 17654 (2008).

[34]S. Derom, R. Vincent, A. Bouhelier, and G. Colas des Francs, Europhys. Lett. **98**, 47008 (2012).